Borneo Journal of Pharmacy
Vol 9 Issue 2 June 2026
Pages 213 – 224

https://journal.umpr.ac.id/index.php/bjop/article/view/11198
DOI: https://doi.org/10.33084/bjop.v9i2.11198
e-ISSN: 2621-4814

Research Article

Integration of Chitosan and *Ageratum conyzoides* Extract in Hydrogel Patches for Enhanced Wound Closure Kinetics under the TIME Framework

Malinda Prihantini [1*]
Yance Anas [2]
Junvidya Heroweti [2]
Dewi Andini Kunti Mulangsri [3]
Wahyudin Bin Jamaludin [4]
Luthfia Mufaridhotun Nahla [5]
Reyhan Raka Mahadika [5]
Fazdilatul Hawa [5]
Nayla Azkya [5]
Rifka Sephia Fassadila [5]

[1] Department of Pharmaceutics and Pharmaceutical Technology, Universitas Wahid Hasyim, Semarang, Central Java, Indonesia
[2] Department of Pharmacology and Clinical Pharmacy, Universitas Wahid Hasyim, Semarang, Central Java, Indonesia
[3] Department of Biology Pharmacy, Universitas Wahid Hasyim, Semarang, Central Java, Indonesia
[4] Department of Pharmacy, Universitas Borneo Lestari, Banjarbaru, South Kalimantan, Indonesia
[5] Department of Pharmacy, Universitas Wahid Hasyim, Semarang, Central Java, Indonesia

[*]email: malindap@unwahas.ac.id; phone: +6285624645411

Keywords:
Ageratum conyzoides
Chitosan
Patch hydrogel
Wound management

Abstract

Chronic wounds pose a significant healthcare challenge in Southeast Asia, with prevalence rates reaching 50.8%. Conventional systemic therapies often fail due to persistent inflammation and bacterial biofilm formation. This study presents a novel approach that combines chitosan, a hydrophilic scaffold that maintains optimal moisture and prevents microbial contamination, with *Ageratum conyzoides*, which is rich in flavonoids with anti-inflammatory and pro-proliferative properties. This study aimed to evaluate the impact of chitosan combined with *A. conyzoides* in a hydrogel patch formulation on wound healing as a comprehensive approach to the TIME (Tissue, Inflammation, Moisture, Epithelization) concept. The standardized plant material was formulated into patches by a solvent-casting method using three extract-to-chitosan ratios: F1 (2:0), F2 (1:1), and F3 (2:1). Evaluation encompassed physical characterization, acute dermal irritation, and wound-healing activity assessment. Plant material met the Indonesian Herbal Pharmacopeia standards, yielding 9.96 ± 0.10% total flavonoid content, with phytochemical screening confirming flavonoids, phenolics, and quinones. All formulations demonstrated favorable physical characteristics: thickness of 0.08–0.11 mm, folding endurance of 64–479 folds, and moisture absorption of 6.12–9.39%, with no acute dermal irritation observed in rabbits. In a 14-day linear incision wound model using male Wistar rats, F3 achieved superior healing efficacy (97% closure, rate constant 0.2972 day^{-1}), reaching 90% closure by day 7.75, significantly outperforming the positive control (Bioplacenton®, 89%) and negative control (79%). These results highlight F3's synergistic effects via anti-inflammatory and proliferative mechanisms, following first-order kinetics and comprehensively addressing the TIME framework to enhance wound healing.

Received: October 21st, 2025
1st Revised: December 24th, 2025
Accepted: March 19th, 2026
Published: June 30th, 2026

INTRODUCTION

Chronic wounds represent a major healthcare burden across Southeast Asia. A systematic review and meta-analysis of epidemiological data spanning 2011 to 2025 across Asia revealed that Southeast Asia exhibits the highest chronic wound

How to cite: Prihantini M, Anas Y, Heroweti J, Mulangsri DAK, Jamaludin WB, Nahla LM, et al. Integration of Chitosan and Ageratum conyzoides Extract in Hydrogel Patches for Enhanced Wound Closure Kinetics under the TIME Framework. Borneo J Pharm. 2026;9(2):213-24. doi:10.33084/bjop.v9i2.11198

prevalence on the continent, reaching 50.8%[1]. Clinical records from Dr. Soetomo Hospital in Surabaya (2015–2020) further indicate that 49% of chronic wound patients were elderly, with 40% presenting with severe exudate and necrotic tissue burden[2]. Multiple pathophysiological barriers, including compromised microvascular perfusion, persistent inflammatory cascades, and recalcitrant bacterial biofilm formation, severely impede chronic wound healing. Consequently, conventional systemic therapies frequently demonstrate limited clinical efficacy while inducing substantial systemic toxicity, particularly in geriatric populations with metabolic dysfunctions and multi-organ comorbidities. Furthermore, the incomplete implementation of the TIME (Tissue management, Infection and inflammation control, Moisture balance, Epithelialization advancement) clinical framework has significantly contributed to prolonged healing times[3]. Therefore, a localized topical preparation that comprehensively addresses all facets of the TIME paradigm is urgently required to accelerate wound closure while ensuring patient compliance and comfort.

Localized topical drug delivery platforms provide controlled active distribution within the wound microenvironment, minimizing systemic adverse effects while maximizing therapeutic accumulation at the target tissue site[4]. Advanced biomaterial delivery systems, such as biomimetic hydrogels, polymeric films, and nanofibers, have demonstrated superior drug retention and enhanced tissue regeneration relative to traditional topical formulations[5]. Among these biomaterials, chitosan, a biocompatible hydrogel-forming polysaccharide derived from crustacean shell waste, serves as an effective scaffold in dressings for deep wounds with partial-thickness skin loss[6].

The intrinsic bioactivity of hydrogel patches can be substantially augmented by incorporating phytochemical extracts endowed with proven tissue-regenerative properties, such as those derived from *Ageratum conyzoides*[7]. Although historically categorized as an invasive agricultural weed responsible for 15% to 42% reductions in rice crop yields[8], *A. conyzoides* exhibits potent anti-inflammatory, antitumor, and wound-healing activities in both incision and diabetic wound models across extract suspension and gel vehicles[9-13]. Phytochemical profiling has revealed a rich spectrum of secondary metabolites in this species, including flavonoids, alkaloids, tannins, quinones, steroids, triterpenoids, sterols, and saponins[14]. Flavonoids constitute the predominant bioactive class, with quercetin, its glycosidic derivatives, and kaempferol serving as major marker compounds[15].

Under the TIME management framework, the chitosan hydrogel matrix acts as a biodegradable, moisture-balancing film providing essential antimicrobial barrier protection, while *A. conyzoides* extract modulates local inflammatory signaling and promotes re-epithelialization. Concurrently, the patch configuration provides an occlusive barrier shielding the wound bed from exogenous environmental contamination while serving as a structural matrix for cell migration[16]. Furthermore, repurposing both chitosan and *A. conyzoides*, materials routinely classified as agricultural and bio-waste, into high-value pharmaceutical products directly aligns with Indonesia's National Asta Cita framework and the Roadmap for Pharmaceutical Raw Material Independence. To date, no investigations have reported the formulation and evaluation of an *A. conyzoides* ethanolic extract embedded within a chitosan hydrogel patch matrix, representing a critical research gap. Accordingly, this study aims to evaluate the wound-healing efficacy of a novel hydrogel patch that combines chitosan with *A. conyzoides* ethanolic extract and is engineered in alignment with the TIME paradigm.

MATERIALS AND METHODS

Materials

The plant material used in this study consisted of fresh *A. conyzoides* herb harvested from agricultural rice fields in Pongangan Village, Gunungpati, Semarang. Pharmaceutical-grade excipients and reagents included 96% ethanol (Bratachem), low-molecular-weight chitosan (Chi Multiguna), polyvinyl alcohol (PVA; Merck), polyethylene glycol 400 (PEG 400; Merck), glycerin (Merck), methylparaben (Sigma-Aldrich), propylparaben (Sigma-Aldrich), and freshly prepared distilled water obtained from the Pharmaceutics and Pharmaceutical Technology Laboratory, Universitas Wahid Hasyim. Analytical-grade reagents, including 96% ethanol, potassium acetate, and aluminum chloride, were procured from Merck. Primary analytical and processing equipment comprised a forced-air drying oven (DHG 9053A), a digital analytical balance (Ohaus), a calibrated digital pH meter (Hanna Instruments HI98107), a temperature-controlled magnetic stirrer (DLAB Scientific), a double-beam UV-Vis spectrophotometer (Shimadzu UV-1800), and standard volumetric glassware (Pyrex).

Methods

Botanical authentication and raw material standardization

Taxonomic identification and botanical authentication of the plant material were performed at the Integrated Laboratory, Faculty of Mathematics and Natural Sciences, Universitas Negeri Semarang (No. 115/UN.37/SHP/ Lab. Taksonomi Tumbuhan/IX/2024), confirming the species identity as *A. conyzoides*. A total of 6.7 kg of freshly harvested *A. conyzoides* herb underwent sequential postharvest processing, including manual sorting, washing with running water, mechanical chopping, shade drying, and dry sorting. The dried herb was pulverized using a mechanical grinder and passed through a 30-mesh sieve to yield 2.0 kg of standardized herbal powder. Raw material quality parameters, including loss on drying, total ash value, water-soluble extractive value, and ethanol-soluble extractive value, were evaluated in accordance with the specifications of the Indonesian Herbal Pharmacopeia[17].

Ethanolic extraction and extract standardization

Standardized *A. conyzoides* powder (500 g) was extracted by cold maceration in 3750 mL of 96% ethanol for 3 days, with intermittent agitation, to obtain filtrate I. Remaceration was conducted on the insoluble residue using 1250 mL of fresh 96% ethanol for an additional 2 days, yielding filtrate II. The combined filtrates were concentrated under reduced pressure at 40°C using a rotary vacuum evaporator until a viscous crude extract was obtained. The extraction yield was calculated and verified to exceed the minimum pharmacopeial benchmark of 9.6%[17]. Phytochemical screening for flavonoids, phenolic constituents, and quinones was performed following the Farnsworth protocol. Total flavonoid content was quantified using a modified spectrophotometric assay standardized against quercetin aglycone rather than rutin, accounting for the predominance of semipolar non-glycosidic flavonoids indicated by the higher ethanol-soluble extractive value relative to the water-soluble fraction[18].

Formulation and preparation of chitosan–A. conyzoides hydrogel patches

Hydrogel patches were formulated by modifying an established hydrogel matrix[19], substituting HPMC with low-molecular-weight chitosan and incorporating *A. conyzoides* ethanolic extract at extract-to-chitosan weight ratios of 2:0 (F1), 1:1 (F2), and 2:1 (F3). The complete formulation compositions are detailed in **Table I**. Patches were fabricated using a solvent-casting method. Polyvinyl alcohol was fully dissolved in distilled water at 80°C under continuous magnetic stirring at 500 rpm. Chitosan was gradually added to the PVA solution to obtain a homogeneous polymeric gel base. Methylparaben and propylparaben, pre-dissolved in a blend of glycerin and PEG 400, were incorporated as humectants and plasticizers. The ethanolic extract of *A. conyzoides*, dissolved in 96% ethanol, was added to the gel base and stirred until completely uniform. Aliquots of 4.0 g were poured into 60 x 15 mm glass petri dishes and dried in a forced-air oven at 45°C for 5 hours. The resulting dried films were carefully peeled from the dishes, wrapped in aluminum foil, sealed in zip-lock bags, and stored in a desiccator containing silica gel before testing[19].

Table I. Quantitative formulation design of chitosan–*A. conyzoides* hydrogel patches (% w/v).

Ingredient	Formula 1 (F1)	Formula 2 (F2)	Formula 3 (F3)
Ageratum conyzoides ethanolic extract	2.0	1.0	2.0
Chitosan	–	1.0	1.0
Polyvinyl alcohol	1.0	1.0	1.0
Polyethylene glycol 400	5.0	5.0	5.0
Methylparaben	0.05	0.05	0.05
Propylparaben	0.15	0.15	0.15
Purified water	q.s. to 100 mL	q.s. to 100 mL	q.s. to 100 mL

Physicochemical characterization of hydrogel patches

Organoleptic properties, including color, odor, physical state, and surface texture, were visually inspected, while film thickness was measured at three distinct coordinates using digital calipers[20]. Mass uniformity was established by individually weighing patches, calculating the mean weight and standard deviation, and verifying that the coefficient of variation remained below 5%[19]. Surface pH was determined using a semi-solid digital pH meter pre-calibrated with standard buffer solutions of pH 4.0 and 7.0[21]. Moisture content was evaluated by weighing 1 cm^2 patch samples (W_1), incubating them in a climatic chamber at 40°C and 75% ± 5% relative humidity for 24 hours, and reweighing them (W_2) to

determine percentage moisture uptake. Folding endurance was tested by repeatedly folding a 4 cm² film along the same central axis up to 500 times or until structural tearing occurred[19].

Acute dermal irritation bioassay

Acute dermal irritation was evaluated on the shaved dorsal skin of healthy rabbits 24 hours post-depilation. Initial screening was performed on a single animal, followed by confirmatory testing on two additional rabbits. Test formulations (2 x 3 cm²) were applied topically to designated skin regions. Primary endpoints, specifically erythema and edema formation, were scored at 1, 24, 48, and 72 hours post-patch removal by certified veterinarians from the Animal Health Center of the Semarang City Agriculture Department[22].

In vivo wound healing efficacy in rats

Healthy male Wistar rats weighing 180–200 g were acclimatized for 5 days under standard laboratory conditions. Animals were randomly assigned to five experimental groups (n = 6 per group). The dorsal fur was shaved, disinfected with 70% ethanol, and topical lidocaine cream was applied for 5 minutes to induce local anesthesia. A linear paravertebral incision measuring 1.0 cm in length and 0.3 cm in depth was surgically created using a sterile scalpel blade. Wounds were covered daily with respective test preparations for 14 consecutive days. Incision length was measured periodically using digital calipers, and percentage wound closure was calculated[23]. The experimental cohorts comprised:

1. Negative Control Group (KP): Treated with placebo patches devoid of chitosan and *A. conyzoides* extract.
2. Positive Control Group (P): Treated topically with commercial Bioplacenton cream.
3. Test Group 1 (F1): Treated with formulation F1 (*A. conyzoides* extract to chitosan ratio of 2:0).
4. Test Group 2 (F2): Treated with formulation F2 (*A. conyzoides* extract to chitosan ratio of 1:1).
5. Test Group 3 (F3): Treated with formulation F3 (*A. conyzoides* extract to chitosan ratio of 2:1).

All animal procedures complied with international ethical standards and were formally approved by the Institutional Ethics Committee of the Faculty of Medicine, Universitas Dian Nuswantoro, Semarang, Indonesia (No. 005320/UNIVERSITAS DIAN NUSWANTORO/2025) issued in 2025.

Data analysis

Qualitative data (organoleptic characteristics, presence of phytochemicals, and dermal irritation scores) were evaluated descriptively. Quantitative data derived from extract yield calculations, flavonoid quantification, patch physical parameters, and *in vivo* wound closure percentages were expressed as mean ± standard deviation. Statistical comparisons across experimental groups were performed using one-way Analysis of Variance (ANOVA) at a 95% confidence level ($\alpha = 0.05$) in SPSS, with post hoc Tukey's HSD test to determine significant differences between formulation groups ($p < 0.05$)[24].

RESULTS AND DISCUSSION

Plant determination confirmed the taxonomic identity of the harvested material as *Ageratum conyzoides* L. Following post-harvest processing of the raw material, standardized pharmacognostic quality parameters were evaluated. The quantitative outcomes are presented in **Table II**.

Table II. Raw material standardization results for *A. conyzoides* herb.

Pharmacognostic Parameter	Experimental Mean	Standard Deviation (±SD)	Indonesian Herbal Pharmacopeia Standard[17]
Non-specific parameters			
Loss on drying (%)	6.36	0.32	<10.0%
Total ash content (%)	5.36	0.49	<12.3%
Specific parameters			
Water-soluble extractive value (%)	16.35	0.11	>11.4%
Ethanol-soluble extractive value (%)	17.26	0.01	>15.4%

The standardization metrics demonstrated that all evaluated physical and chemical parameters strictly complied with the quality specifications outlined in the Indonesian Herbal Pharmacopeia[17]. Loss on drying quantifies the proportion of water

vapor and volatile compounds (such as essential oils) that evaporate at 105°C. Reducing moisture content decreases water activity (a_w) as free water within the plant matrix evaporates, thereby suppressing microbial proliferation and inactivating degradation enzymes[25]. Total ash content met pharmacopeial limits, indicating minimal contamination by inorganic extraneous matter such as soil, sand, or metallic residues, and confirming the thoroughness of the preliminary washing and drying steps[26].

The elevated water-soluble (16.35%) and ethanol-soluble (17.26%) extractive values observed in *A. conyzoides* herb reflect an abundance of phytochemical metabolites extractable by polar and semipolar solvents. The higher yield of ethanol-soluble extractives relative to the water-soluble fraction indicates that the predominant secondary metabolites are semipolar in nature, including flavonoid aglycones, tannins, alkaloids, and non-glycosidic phenolic compounds lacking sugar moieties[25]. These results align closely with prior pharmacognostic evaluations. Compared to Warsinah and Baroroh[26], who reported a loss on drying of 6.21% ± 0.36% and total ash of 1.58% ± 0.42% for foliar simplicia, the present findings exhibit comparable drying efficiency but elevated mineral residue, likely driven by edaphic factors or harvest maturity. Conversely, Shailajan *et al*.[27] documented a higher loss on drying (10.76% ± 0.17%) and total ash (12.06% ± 0.36%), alongside ethanol-soluble extractive values (18.69% ± 1.19%) comparable to the present study, underscoring varietal and environmental influences while confirming high solubilization potential.

The ethanolic extraction of *A. conyzoides* herb yielded a 15.0% recovery, significantly exceeding the minimum pharmacopeial requirement of 9.6%[17]. The standardized quality attributes of the concentrated extract are summarized in **Table III**. Qualitative screening confirmed the presence of three major secondary metabolite classes: flavonoids, phenolics, and quinones. Flavonoids produced a characteristic orange-to-pink color reaction (+), representing the predominant bioactive class reported across *A. conyzoides* literature. Phenolic compounds yielded a deep blue ink-like precipitate (+), indicating a high concentration of polyphenolic structures. These results align with prior phytochemical profiles reported by Maulidya *et al*.[28] and subsequent investigations[29], which identified alkaloids, flavonoids, saponins, tannins, phenolics, and steroids/triterpenoids in *A. conyzoides* foliar extracts. Variations in secondary metabolite distribution are primarily driven by geographical location, soil composition, and environmental stress factors[30].

Table III. Standardization and phytochemical screening outcomes of *A. conyzoides* ethanolic extract.

Quality Parameter	Experimental Result	Pharmacopeial Standard / Reference[17]
Organoleptic inspection	Thick extract, blackish-green color, characteristic *A. conyzoides* odor, bitter with astringent taste	Thick extract, blackish-green color, characteristic *A. conyzoides* odor, bitter with astringent taste
Phytochemical screening		
Flavonoids	+	Orange-to-pink color formation
Phenolics	+	Blue ink-like precipitate formation
Quinones	+	Red color formation
Total flavonoid content (%)	9.96 ± 0.10	>1.40% w/w

Note: (+) = positive for secondary metabolite class.

The total flavonoid content of 9.96% w/w is substantially higher than values reported in previous studies. Dores *et al*.[31] documented flavonoid levels of 5.7263 µg/mL, while reported concentrations ranged from 2.678 mg quercetin equivalents (QE)/g (0.27%) to 78.229 mg QE/g (7.82%), depending on the extraction method and solvent polarity. The elevated flavonoid yield underscores strong radical-scavenging potential, as flavonoids neutralize reactive oxygen species (ROS) through hydrogen atom or electron donation[32]. This intrinsic antioxidant capacity drives the anti-inflammatory, antimicrobial, and tissue-regenerative activities of *A. conyzoides*.

The concentrated ethanolic extract was formulated into transdermal hydrogel patches using solvent-casting techniques, as shown in **Figure 1**. All patch preparations exhibited the characteristic herbal aroma of *A. conyzoides*. Formulations F1 and F3, containing 2% extract, presented a vibrant yellow coloration, whereas F2 (1% extract) appeared brownish-yellow, demonstrating that extract loading directly modulates film opacity and color intensity. Patch texture varied with polymer composition: F1 (devoid of chitosan) was rigid and dry, reflecting the mechanical stiffness of polyvinyl alcohol (PVA) as the sole film-former. Conversely, F2 (1:1 chitosan:PVA ratio) presented a soft, pliable texture with moderate moisture retention, while F3 (2:1 chitosan:PVA ratio) exhibited the softest, most hydrated matrix. These physical trends correlate with the hydrophilic nature of chitosan, a natural polysaccharide that promotes water uptake, whereas PVA imparts structural

rigidity with less intrinsic moisture retention. Quantitative physicochemical properties across all three formulations are compiled in **Table IV**.

a **b** **c**

Figure 1. Physical appearance of *A. conyzoides* extract–chitosan patches: (**a**) F1, (**b**) F, and (**c**) F3.

Table IV. Physicochemical properties of formulated hydrogel patches.

Evaluation Parameter	F1	F2	F3
Weight uniformity (g)	0.50 ± 0.02*	0.62 ± 0.01*	0.64 ± 0.02*
Folding endurance (folds)	64.33 ± 34.00*	268.33 ± 168.00	478.67 ± 30.00*
Film thickness (mm)	0.08 ± 0.96*	0.10 ± 0.95	0.11 ± 0.95*
Moisture absorption (%)	9.39 ± 0.71*	6.12 ± 0.46	7.67 ± 0.76*

Note: Data expressed as mean ± standard deviation (n=3). * Indicates statistical significance ($p < 0.05$).

Patch masses ranged from 0.50 to 0.64 g, meeting commercial transdermal standards (0.40–0.80 g). The higher mass observed in F2 and F3 stems from the inclusion of chitosan, which has a higher bulk density than PVA, consistent with findings by Chopra *et al.*[33]. A folding endurance exceeding 200 folds is required for transdermal patches to prevent structural cracking during application and movement. Formulation F1 (PVA alone) achieved only ~64-fold, failing this benchmark. Incorporating 1% w/w chitosan in F2 increased folding endurance to ~268 folds, while F3 reached ~479 folds, highlighting the role of chitosan in enhancing film flexibility and tensile strength. As noted by Chen and Taguchi[34], extensive hydrogen bonding within the chitosan network and intermolecular interactions between chitosan amine groups and PVA hydroxyl groups yield a resilient, flexible matrix.

Patch thickness (0.08–0.11 mm) complied with standard transdermal dimensions (0.05–0.15 mm), balancing mechanical strength and drug permeability. Chitosan's hygroscopicity contributed to slight increases in thickness; however, once co-crosslinked with PVA, the film resisted excessive swelling[35]. Moisture absorption tests showed that F1 absorbed ~9.4% water, whereas F2 and F3 absorbed 6.1%–7.7%, reflecting a denser film structure in chitosan-containing matrices. These absorption levels fall within the optimal 5%–15% range for wound dressings, maintaining a moist microenvironment aligned with the TIME framework.

Acute dermal irritation testing on rabbit skin (**Figure 2**) produced no detectable erythema or edema at 1, 24, 48, or 72 hours post-application, establishing the local safety of all formulations. *In vivo* wound-healing assessments (**Figure 3**) demonstrated statistically significant differences in wound area reduction among the formulations F1–F3, the positive control (Bioplacenton), and the negative control (placebo patch). Formulation F3 achieved the highest wound closure (97.0% reduction). Relative to the negative control, F1 accelerated wound closure by 1.16-fold and surpassed Bioplacenton by 1.03-fold. Formulation F2 enhanced healing by 1.18-fold compared with the negative control and by 1.05-fold compared with Bioplacenton. Formulation F3 yielded the highest enhancements, achieving 1.23-fold and 1.09-fold increases, respectively. These results confirm that *A. conyzoides* extract serves as the primary driver of tissue repair, with chitosan providing synergistic functional support.

The wound-healing performance of F1–F3 proved superior to outcomes reported by Sahila *et al.*[36], who evaluated an *A. conyzoides* extract gel in diabetic wound models and recorded 62.74% closure in test groups, 51.77% in positive controls, and 41.65% in negative controls. The therapeutic efficacy of *A. conyzoides* is driven by its main flavonoids, quercetin and kaempferol, which exert potent antioxidant effects and stimulate fibroblast proliferation[13]. These flavonoids scavenge ROS, including superoxide anions, hydrogen peroxide, hydroxyl radicals, and peroxyl radicals, and chelate transition metal ions (Fe^{2+} and Cu^{2+}) to inhibit Fenton-mediated radical generation. Furthermore, flavonoids downregulate ROS-generating enzymes, such as xanthine oxidase and NADPH oxidase, suppressing oxidative stress at the cellular level[37,38].

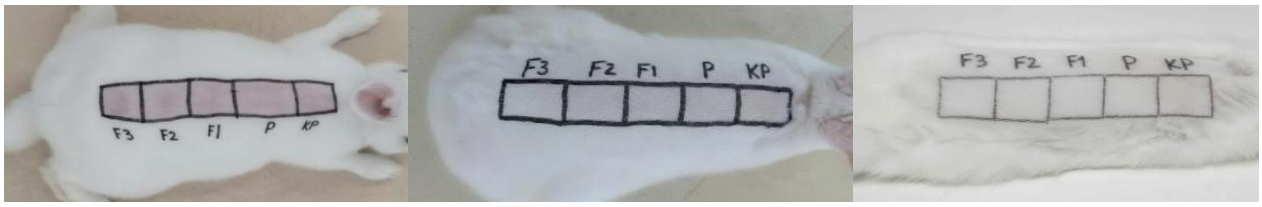

a **b** **c**

Figure 2. Acute dermal irritation test results in rabbits at 72 hours post-patch removal: F3, F2, F1, P (Bioplacenton positive control), and KP (placebo patch negative control) across (**a**) Rabbit 1, (**b**) Rabbit 2, and (**c**) Rabbit 3.

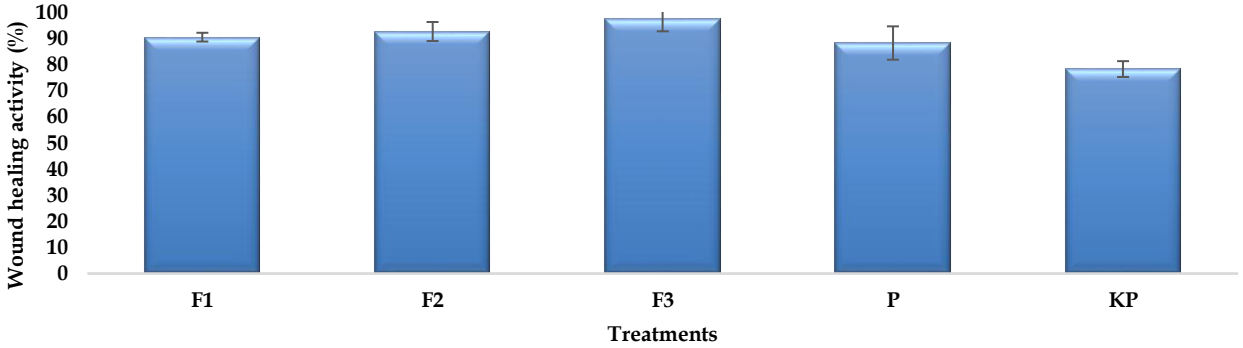

Figure 3. Representative wound closure photographs at day 14 across experimental groups: F1, F2, F3, P (Bioplacenton positive control), and KP (placebo negative control).

Elevated flavonoid levels activate the nuclear factor erythroid 2–related factor 2 (Nrf2) / antioxidant response element (ARE) signaling pathway, a central regulator of cellular antioxidant defenses. Nrf2 activation upregulates downstream phase II enzymes, including superoxide dismutase (SOD), which catalyzes the dismutation of H_2O_2; catalase (CAT), which decomposes H_2O_2 into H_2O and O_2; glutathione peroxidase (GPx), which reduces lipid hydroperoxides; and glutathione S-transferase (GST). Studies evaluating rutin demonstrate that Nrf2 activation restores depleted levels of reduced glutathione (GSH), CAT, and SOD during oxidative stress while reducing malondialdehyde (MDA) levels, a marker of lipid peroxidation[39].

To evaluate tissue restoration rates, serial wound surface measurements were monitored over 14 days, as illustrated in **Figure 4**. By day 3, the negative control cohort retained ~80% of the initial wound surface area, whereas the treated groups exhibited rapid contraction (~50%). By day 14, residual wound areas were lowest in F3 (~3.0%), followed by F2 (~7.0%) and F1 (~9.0%), compared with the positive control (~12.0%) and the negative control (~22.0%). All patch formulations accelerated tissue closure without an initial lag phase. Quantitative kinetic parameters derived from kinetic modeling are summarized in **Table V**.

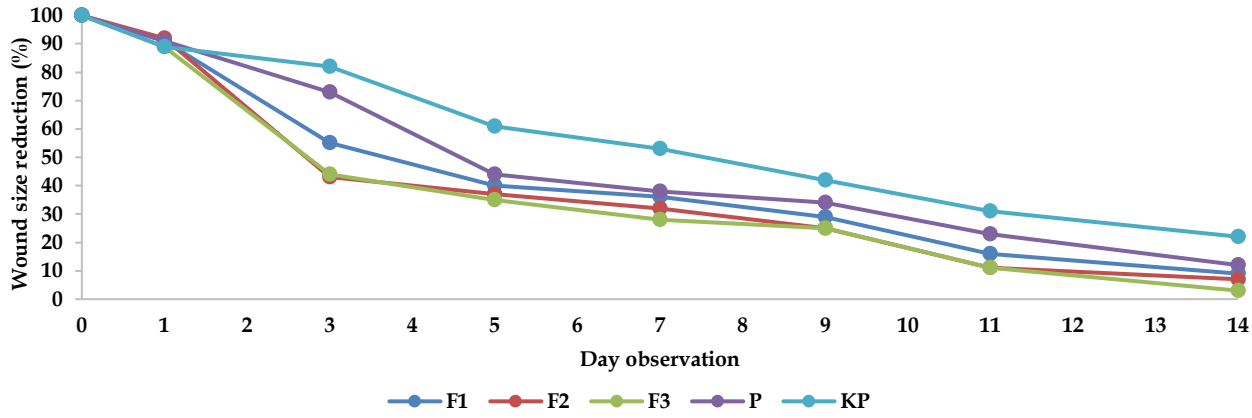

Figure 4. Serial percentage residual wound area curves over 14 days across experimental cohorts (F1, F2, F3, P, and KP).

Based on high coefficients of determination ($R^2 > 0.98$), wound closure across all cohorts conforms to first-order kinetic decay, described by the logarithmic rate **Equation 1**, where A_0 represents initial wound area, A_t represents wound area at time t, and rate constant (k) represents the first-order rate constant (day^{-1}). First-order kinetics align with the physiological stages of wound repair, where rapid tissue contraction during hemostasis, inflammation, and early proliferation slows as the tissue enters late remodeling[40]. The k confirms that F3 achieved the highest healing rate (0.2972 day^{-1}), followed by F2, F1, P, and KP. Formulations F1, F2, and F3 achieved 50% closure ($t_{1/2}$) within 2.33 to 3.84 days and 90% closure (t_{90}) within 7.75 to 12.74 days, substantially faster than the 28.45 days required for positive control and 53.54 days for negative control[4]. The time required for t_{90} in F2 (8.84 days) was 1.44-fold shorter than in F1 (12.74 days) and decreased further in F3 (7.75 days), confirming that incorporating *A. conyzoides* extract into a chitosan hydrogel matrix significantly accelerates healing relative to single-polymer controls.

Table V. Mathematical kinetic parameters of wound closure across treatment groups.

Experimental Group	k (day^{-1})	$t_{1/2}$ (days)	t_{90} (days)	Coefficient of Determination (R^2)
Formula 1 (F1)	0.1807	3.84	12.74	0.9881
Formula 2 (F2)	0.2606	2.66	8.84	0.9811
Formula 3 (F3)	0.2972	2.33	7.75	0.9818
Positive control (P)	0.0809	8.56	28.45	0.9947
Negative control (KP)	0.0430	16.12	53.54	0.9984

$$\ln(A_t) = \ln(A_0) - kt \qquad [1]$$

The wound-healing efficacy of *A. conyzoides* hydrogel patches is driven by its active flavonoids, quercetin and kaempferol, which modulate key regenerative signaling pathways[41]. Primarily, these flavonoids upregulate transforming growth factor-β (TGF-β) expression, an essential regulator of keratinocyte migration, re-epithelialization, inflammation, angiogenesis, and matrix formation, and stimulate type I collagen synthesis via Smad2/3 phosphorylation[42]. Concurrently, they enhance the expression of vascular endothelial growth factor-C (VEGF-C) and Ang-1/Tie-2, promoting neovascularization, in which enhanced capillary formation restores microvascular perfusion, delivering essential oxygen, nutrients, and repair cells directly to the regenerating tissue bed. Furthermore, these flavonoid constituents activate mitogen-activated protein kinase (MAPK) and extracellular signal-regulated kinase (ERK) signaling cascades, effectively regulating cellular proliferation, directional migration, and functional differentiation within the wound environment[43].

Across the four stages of wound repair (hemostasis, inflammation, proliferation, and remodeling), flavonoids exert targeted therapeutic effects. During inflammation, flavonoids inhibit nuclear factor-kappa B (NF-κB) activation, shifting macrophages from a pro-inflammatory M1 phenotype to an anti-inflammatory M2 phenotype. This transition downregulates pro-inflammatory cytokines (IL-1β, IL-6, TNF-α) while upregulating anti-inflammatory mediators[44]. During proliferation, quercetin and kaempferol accelerate fibroblast migration, stimulate TGF-β signaling, downregulate matrix metalloproteinase-9 (MMP-9), and maintain extracellular matrix (ECM) homeostasis, thereby preventing chronic non-healing wound states[37]. In summary, the *A. conyzoides* extract incorporated within the chitosan hydrogel patch operates through a multi-target mechanism encompassing restoration of redox balance via ROS scavenging and Nrf2/ARE activation, resolution of persistent inflammation through M_1-to-M_2 macrophage polarization, stimulation of keratinocyte and fibroblast proliferation, enhancement of VEGF-driven angiogenesis, and regulation of ECM synthesis and remodeling during final tissue maturation.

CONCLUSION

This study successfully formulated and evaluated a novel chitosan–*A. conyzoides* extract hydrogel patch as an effective topical wound-healing delivery system. Formulation F3 (2:1 extract-to-chitosan ratio) demonstrated superior therapeutic efficacy, achieving 97% wound closure at day 14 and significantly outperforming both the commercial positive control (Bioplacenton, 89%) and the placebo negative control (79%). Quantitative kinetic modeling established that wound repair followed first-order decay kinetics at 0.2972 day-1, exhibiting a half-life of 2.33 days and achieving 90% closure by day 7.75, confirming rapid therapeutic onset without an initial lag phase. This enhanced regenerative performance stems from the functional synergy between the chitosan hydrogel matrix, which acts as a biocompatible, moisture-balancing scaffold

providing antimicrobial protection, and the high flavonoid content of *A. conyzoides* extract, which restores redox homeostasis, suppresses chronic inflammation via macrophage M_1-to-M_2 phenotype modulation, and accelerates tissue repair through TGF-β/Smad, VEGF-mediated angiogenesis, and MAPK/ERK signaling cascades. All patch formulations exhibited favorable physicochemical properties, showed no dermal irritation in rabbit models, and satisfied all criteria of the TIME clinical paradigm for wound management. Future investigations should evaluate long-term physical stability, *in vivo* efficacy in chronic non-healing wound models (such as diabetic ulcers), and percutaneous release kinetics to optimize clinical performance and advance the sustainable utilization of bio-waste materials for pharmaceutical independence.

ACKNOWLEDGMENT

The authors express their sincere gratitude to Universitas Wahid Hasyim for providing financial support for this study through the Competitive DIPA Research Grant for Fiscal Year 2024, coordinated by the Research and Community Service Institute. Gratitude is also extended to the Faculty of Pharmacy, Universitas Wahid Hasyim, for providing essential laboratory facilities and technical infrastructure, and to all individuals whose expertise, technical assistance, and valuable contributions enabled the successful execution of this research.

AUTHORS' CONTRIBUTION

Conceptualization: Malinda Prihantini, Yance Anas, Junvidya Heroweti, Dewi Andini Kunti Mulangsri
Data curation: Malinda Prihantini, Luthfia Mufaridhotun Nahla, Reyhan Raka Mahadika, Fazdilatul Hawa, Nayla Azkya, Rifka Sephia Fassadila
Formal analysis: Malinda Prihantini, Yance Anas, Junvidya Heroweti, Dewi Andini Kunti Mulangsri, Wahyudin Bin Jamaludin
Funding acquisition: Malinda Prihantini
Investigation: Malinda Prihantini, Luthfia Mufaridhotun Nahla, Reyhan Raka Mahadika, Fazdilatul Hawa, Nayla Azkya, Rifka Sephia Fassadila
Methodology: Malinda Prihantini, Yance Anas, Junvidya Heroweti, Dewi Andini Kunti Mulangsri
Project administration: Malinda Prihantini
Resources: -
Software: Malinda Prihantini
Supervision: Malinda Prihantini, Yance Anas, Junvidya Heroweti, Dewi Andini Kunti Mulangsri, Wahyudin Bin Jamaludin
Validation: Malinda Prihantini, Yance Anas, Junvidya Heroweti, Dewi Andini Kunti Mulangsri, Wahyudin Bin Jamaludin
Visualization: Malinda Prihantini
Writing - original draft: Malinda Prihantini, Luthfia Mufaridhotun Nahla, Reyhan Raka Mahadika, Fazdilatul Hawa, Nayla Azkya, Rifka Sephia Fassadila
Writing - review & editing: Malinda Prihantini, Yance Anas, Junvidya Heroweti, Dewi Andini Kunti Mulangsri, Wahyudin Bin Jamaludin

DATA AVAILABILITY

None.

CONFLICT OF INTEREST

The authors declare no conflicts of interest related to this study.

REFERENCES

1. Burhan A, Syafiqah N, Ruangdet K, Oanh LTK, MacLeod ER, Roy AD, et al. Hidden Wounds: Prevalence of Chronic Wounds in Asia, A Systematic Review and Meta-Analysis. Java Nurs J. 2025;3(3):221-35. DOI: 10.61716/jnj.v3i3.117.

2. Budirahmadina NA, Perdanakusuma DS, Ervianti E, Saputra ID. The Clinical Profile of Patients with Chronic Wounds at Dr. Soetomo General Hospital 2015-2020. Berkala Ilmu Kesehatan Kulit Kelamin. 2023;35(1):57-66. DOI: 10.20473/bikk.V35.1.2023.57-66.

3. Fakher S, Westenberg D. A Comprehensive Overview of Chronic Wound Infections and Current Treatment Methods. Wound Repair Regen. 2025;33(6):e70115. DOI: 10.1111/wrr.70115; PMID: 41292174.

4. Hosseini SA, Noruzi S, Kesharwani P, Sahebkar A. Hydrogel-based dressing for wound healing: A systematic review of clinical trials. Int J Biol Macromol. 2025;308(Pt 1):142322. DOI: 10.1016/j.ijbiomac.2025.142322; PMID: 40118421.

5. Feng L, Shi Y, Wang Z, Wang C, Fan Y, Wang N, et al. A review of biomimetic hydrogel wound dressings: Design inspiration, construction strategies, multifunctionality and applications. Int J Biol Macromol. 2025;328(Pt 1):147475. DOI: 10.1016/j.ijbiomac.2025.147475; PMID: 40915457.

6. Feng P, Luo Y, Ke C, Qiu H, Wang W, Zhu Y, et al. Chitosan-Based Functional Materials for Skin Wound Repair: Mechanisms and Applications. Front Bioeng Biotechnol. 2021;9:650598. DOI: 10.3389/fbioe.2021.650598; PMID: 33681176; PMCID: PMC7931995.

7. Arulprakash K, Murugan R, Ponrasu T, Iyappan K, Gayathri VS, Suguna L. Efficacy of Ageratum conyzoides on tissue repair and collagen formation in rats. Clin Exp Dermatol. 2012;37(4):418-24. DOI: 10.1111/j.1365-2230.2011.04285.x; PMID: 22452483.

8. Negi B, Khatri K, Bargali SS, Bargali K. Invasive Ageratina adenophora (Asteraceae) in Agroecosystems of Kumaun Himalaya, India: A Threat to Plant Diversity and Sustainable Crop Yield. Sustainability. 2023;15(14):10748. DOI: 10.3390/su151410748.

9. Lobot R, Datu O, Maarisit W, Tumbel S. Uji Efektivitas Ekstrak Etanol Daun Bandotan A. conyzoides L Sebagai Hemostatis Terhadap Luka Potong Pada Tikus Putih. Biofarmasetikal Trop Trop J Biopharm. 2019;1(1):13-7. DOI: 10.55724/jbiofartrop.v1i1.30.

10. Saputri MP, Utami R, Fadila J, Handayani SN. Anti-inflammation Activity of A. conyzoides Leaf Ethanol Extract on Rattus Norvegicus. Walisongo J Chem. 2020;3(1):46-51. DOI: 10.21580/wjc.v3i1.6136.

11. Chahal R, Nanda A, Akkol EK, Sobarzo-Sánchez E, Arya A, Kaushik D, et al. *Ageratum conyzoides* L. and Its Secondary Metabolites in the Management of Different Fungal Pathogens. Molecules. 2021;26(10):2933. DOI: 10.3390/molecules26102933; PMID: 34069197; PMCID: PMC8156077.

12. Lin Z, Lin Y, Shen J, Jiang M, Hou Y. Flavonoids in Ageratum conyzoides L. Exert Potent Antitumor Effects on Human Cervical Adenocarcinoma HeLa Cells In Vitro and In Vivo. Biomed Res Int. 2020;2020:2696350. DOI: 10.1155/2020/2696350; PMID: 32461974; PMCID: PMC7218960.

13. Sukmawan YP, Alifiar I, Nurdianti L, Ningsih WR. Wound Healing Effectivity of the Ethanolic Extracts of Ageratum conyzoides L. Leaf (White and Purple Flower Type) and Centella asiatica and Astaxanthin Combination Gel Preparation in Animal Model. Turk J Pharm Sci. 2021;18(5):609-15. DOI: 10.4274/tjps.galenos.2021.34676; PMID: 34719189; PMCID: PMC8562118.

14. Mutingatun S, Fachriyah E, Kusrini D. Isolation, Identification, and Antioxidant Activity of Flavonoid Compounds in the Ethanol Extract in Bandotan Leaves (A. conyzoides). J Kimia Sains Aplikasi. 2022;25(12):456-66. DOI: 10.14710/jksa.25.12.456-466.

15. Jan R, Khan M, Asaf S, Lubna, Asif S, Kim KM. Bioactivity and Therapeutic Potential of Kaempferol and Quercetin: New Insights for Plant and Human Health. Plants. 2022;11(19):2623. DOI: 10.3390/plants11192623; PMID: 36235488; PMCID: PMC9571405.

16. Jeong WY, Kwon M, Choi HE, Kim KS. Recent advances in transdermal drug delivery systems: a review. Biomater Res. 2021;25(1):24. DOI: 10.1186/s40824-021-00226-6; PMID: 34321111; PMCID: PMC8317283.

17. Kementerian Kesehatan Republik Indonesia. Farmakope Herbal Indonesia Edisi II. Jakarta: Kementerian Kesehatan Republik Indonesia; 2017.

18. Tiranakwit T, Puangpun W, Tamprasit K, Wichai N, Siriamornpun S, Srisongkram T, et al. Phytochemical Screening on Phenolic, Flavonoid Contents, and Antioxidant Activities of Six Indigenous Plants Used in Traditional Thai Medicine. Int J Mol Sci. 2023;24(17):13425. DOI: 10.3390/ijms241713425; PMID: 37686230; PMCID: PMC10487580.

19. Suwandecha T, Changklang P. Formulation development and characterization of a transdermal patch containing Crinum asiaticum leaves extract. J Appl Pharm Sci. 2023;13(12):207-13. DOI: 10.7324/japs.2023.151643.

20. Kongkwamcharoen C, Itharat A, Ketjinda W, Lee HY, Moon GS, Davies NM. Formulation design and physicochemical evaluation of an anti-inflammatory hydrogel patch containing Crinum asiaticum L. extract. Res Pharm Sci. 2023;18(3):244-61. DOI: 10.4103/1735-5362.371581; PMID: 37593159; PMCID: PMC10427795.

21. Al-Farhan W, Abusara OH, Abu-Sini M, Hikmat S, Tarawneh O, Al-Kouz S, et al. Development, Characterization, and Biological Evaluation of a Self-Healing Hydrogel Patch Loaded with Ciprofloxacin for Wound Dressings. Polymers. 2025;17(19):2686. DOI: 10.3390/polym17192686; PMID: 41096331; PMCID: PMC12527037.

22. Wang J, Li Z, Sun F, Tang S, Zhang S, Lv P, et al. Evaluation of dermal irritation and skin sensitization due to vitacoxib. Toxicol Rep. 2017;4:287-90. DOI: 10.1016/j.toxrep.2017.06.003; PMID: 28959651; PMCID: PMC5615138.

23. Rusnedy R, Febrina M, Sari CP. Uji Aktivitas Wound Healing Ekstrak Etanol Buah Averrhoa bilimbiL. (Belimbing Wuluh) pada Mencit Putih Jantan (Mus musculus). Pharmacon J Farmasi Indones. 2023;20(1):50-60. DOI: 10.23917/pharmacon.v20i1.22677.

24. Chiangnoon R, Samee W, Uttayarat P, Jittachai W, Ruksiriwanich W, Sommano SR, et al. Phytochemical Analysis, Antioxidant, and Wound Healing Activity of Pluchea indica L. (Less) Branch Extract Nanoparticles. Molecules. 2022;27(3):635. DOI: 10.3390/molecules27030635; PMID: 35163900; PMCID: PMC8839647.

25. Oliveira-Alves SC, Andrade F, Prazeres I, Silva AB, Capelo J, Duarte B, et al. Impact of Drying Processes on the Nutritional Composition, Volatile Profile, Phytochemical Content and Bioactivity of Salicornia ramosissima J. Woods. Antioxidants. 2021;10(8):1312. DOI: 10.3390/antiox10081312. PMID: 34439560; PMCID: PMC8389250.

26. Warsinah, Baroroh HN. Pharmacognostic Profile of A. conyzoides L Plant and Simplicia. Pharmacogn J. 2020;12(5):1072-6. DOI: 10.5530/pj.2020.12.151.

27. Shailajan S, Wadke P, Joshi H, Tiwari B. Evaluation of quality and efficacy of an ethnomedicinal plant Ageratum conyzoides L. in the management of pediculosis. J Young Pharm. 2013;5(4):139-43. DOI: 10.1016/j.jyp.2013.10.005; PMID: 24563592; PMCID: PMC3930115.

28. Maulidya SAI, Nuari DA, Suryana S, Almarifah S. Antibacterial Activity of Bandotan (A. conyzoides L) Leaves Extracts Against Methicillin-Resistant Staphylococcus aureus. Borneo J Pharm. 2020;3(4):243-8. DOI: 10.33084/bjop.v3i4.1552.

29. Bafadal M. Potensi Daun Bandotan (Ageratum conyzoides L.) Terhadap Biofilm Streptococcus pyogenes. J Sains Kes. 2025;6(1):32-40. DOI: 10.30872/jsk.v6i1.653.

30. Labarrere B, Prinzing A, Dorey T, Chesneau E, Hennion F. Variations of Secondary Metabolites among Natural Populations of Sub-Antarctic Ranunculus Species Suggest Functional Redundancy and Versatility. Plants. 2019;8(7):234. DOI: 10.3390/plants8070234; PMID: 31331007; PMCID: PMC6681328.

31. Dores RG, Guimarães SF, Braga TV, Fonseca MC, Martins PM, Ferreira TC. Phenolic compounds, flavonoids and antioxidant activity of leaves, flowers and roots of goat weed. Hortic Bras. 2014;32(4):486-90. DOI: 10.1590/S0102-053620140000400019.

32. Zahra M, Abrahamse H, George BP. Flavonoids: Antioxidant Powerhouses and Their Role in Nanomedicine. Antioxidants. 2024;13(8):922. DOI: 10.3390/antiox13080922; PMID: 39199168; PMCID: PMC11351814.

33. Chopra H, Bibi S, Kumar S, Khan MS, Kumar P, Singh I. Preparation and Evaluation of Chitosan/PVA Based Hydrogel Films Loaded with Honey for Wound Healing Application. Gels. 2022;8(2):111. DOI: 10.3390/gels8020111; PMID: 35200493; PMCID: PMC8871709.

34. Chen X, Taguchi T. Enhanced Skin Adhesive Property of Hydrophobically Modified Poly(vinyl alcohol) Films. ACS Omega. 2020;5(3):1519-27. DOI: 10.1021/acsomega.9b03305; PMID: 32010825; PMCID: PMC6990645.

35. Huang Y, Zheng J, Zeng G, Xu H, Lv Y, Liang X, et al. Chitosan-crosslinked polyvinyl alcohol anti-swelling hydrogel designed to prevent abdominal wall adhesion. Mater Today Bio. 2023;24:100931. DOI: 10.1016/j.mtbio.2023.100931; PMID: 38234460; PMCID: PMC10792486.

36. Sahila S, Suhendy H, Sukmawan YP. Wound Healing Effectivity of A. conyzoides L. Leaf Ethanolic Extract (Purple Flower Type), Centella asiatica (L.) Urban Leaf Ethanolic Extract, and Astaxanthin Combination Gel Preparation in Diabetic Animal Model. J Farmasi Sains Komunitas J Pharm Sci Community. 2023;20(1):78-83. DOI: 10.24071/jpsc.003319.

37. Huang W, Zhong Y, Gao B, Zheng B, Liu Y. Nrf2-mediated therapeutic effects of dietary flavones in different diseases. Front Pharmacol. 2023;14:1240433. DOI: 10.3389/fphar.2023.1240433; PMID: 37767395; PMCID: PMC10520786.

38. Huang HC, Chen Y, Hu J, Guo XT, Zhou SR, Yang QQ, et al. Quercetin and its derivatives for wound healing in rats/mice: Evidence from animal studies and insight into molecular mechanisms. Int Wound J. 2024;21(2):e14389. DOI: 10.1111/iwj.14389; PMID: 37818786; PMCID: PMC10828129.

39. Naseeb M, Albajri E, Almasaudi A, Alamri T, Niyazi HA, Aljaouni S, et al. Rutin Promotes Wound Healing by Inhibiting Oxidative Stress and Inflammation in Metformin-Controlled Diabetes in Rats. ACS Omega. 2024;9(30):32394-406. DOI: 10.1021/acsomega.3c05595; PMID: 39100330; PMCID: PMC11292823.

40. Watson SI, Gkini E, Bishop J, Scandrett K, Napit I, Lilford RJ. Modelling wound area in studies of wound healing interventions. BMC Med Res Methodol. 2024;24(1):206. DOI: 10.1186/s12874-024-02326-y; PMID: 39285279; PMCID: PMC11403831.

41. Zulkefli N, Zahari CNMC, Sayuti NH, Kamarudin AA, Saad N, Hamezah HS, et al. Flavonoids as Potential Wound-Healing Molecules: Emphasis on Pathways Perspective. Int J Mol Sci. 2023;24(5):4607. DOI: 10.3390/ijms24054607; PMID: 36902038; PMCID: PMC10003005.

42. Arif J, Nasution AN, Nasution SW, Widowati W, Dewi NSM, Kusuma HSW. Antioxidant Activities and Potential Wound Healing Effects of Meniran (Phyllanthus niruri) Extract Gel. Folia Med Indones. 2024;60(1):69-77. DOI: 10.20473/fmi.v60i1.42396.

43. Ukaegbu K, Allen E, Svoboda KKH. Reactive Oxygen Species and Antioxidants in Wound Healing: Mechanisms and Therapeutic Potential. Int Wound J. 2025;22(5):e70330. DOI: 10.1111/iwj.70330. PMID: 40288766; PMCID: PMC12034374.

44. Jomova K, Alomar SY, Valko R, Liska J, Nepovimova E, Kuca K, et al. Flavonoids and their role in oxidative stress, inflammation, and human diseases. Chem Biol Interact. 2025;413:111489. DOI: 10.1016/j.cbi.2025.111489; PMID: 40147618.